Replicative age negatively influences proliferative capacity since early stages in a Whi5-dependent manner

Irene Delgado-Román, Lidia Delgado-Ramos, Sebastián Chávez and Mari Cruz Muñoz Centeno*

Instituto de Biomedicina de Sevilla, Universidad de Sevilla-CSIC-Hospital Universitario V. del Rocío, and Departamento de Genética, Facultad de Biología, Universidad de Sevilla, Seville, E-41012, Spain.

* Corresponding author

Abstract

Clonal cultures exhibit phenotypic variation in spite of being composed of genetically identical cells under equal environmental conditions. Proliferation rate is one of the characters that have been described to show this heterogeneity, but the mechanisms underlying this phenomenon are still poorly understood. Cell cycle regulation controls proliferative capacity and previous transcriptomic studies revealed that budding yeast microcolonies with low proliferation rates display high levels of the G1-S transition inhibitor Whi5. This regulator, which, in budding yeast, plays a similar role as Retinoblastoma protein in mammalian cells, has been also linked to replicative aging in late steps of mother cells lifespan. In this work, we combined single cell microencapsulation with confocal microscopy to study heterogeneity in clonal cultures. Using this new method, we found that a significant proportion of slow-growing microcolonies are founded by mother cells with a short number of cell cycles. We also found that the reduction in the proliferation capacity of microcolonies founded by young mother cells is related to the expression levels of Whi5, which increases with mother cell age since early stages. Our results establish that stably reduced proliferation is not exclusively linked to old mother cells and indicate that cell age contributes to proliferation heterogeneity by modulating cell cycle regulation.

Introduction

Heterogeneity can be defined as the presence of different features within a population (Ackermann, 2015; Ryall et al., 2012; Sánchez-Romero & Casadesús, 2014). Differences among cells within the same clonal culture can arise by mutations accumulated during population growth. In addition to this genetic heterogeneity, which is relatively well understood (Cota et al., 2012; Davis & Isberg, 2016; Ghosh et al., 2020; Olivenza et al., 2019; Sampaio & Dunlop, 2020; Ziv et al., 2013), there is also phenotypical heterogeneity, observed in isogenic populations, that does not depend on mutations or environmental changes. In this latter case, heterogeneity can be present in any aspect of cell phenotype, like shape, size or differential expression of particular genes (J. A. Lee et al., 2019; Levy et al., 2012; Martins & Locke, 2015; Newman et al., 2006). Phenotypical heterogeneity can also deal with the capacity of isogenic cells to divide and proliferate.

Proliferative heterogeneity explains variations in growth rate within a cell culture, as it has been repeatedly observed in the budding yeast *Saccharomyces cerevisiae* (García-Martínez et al., 2016; Levy et al., 2012). We have previously described that encapsulation of single cells from a yeast clonal population in alginate microspheres produce a wide range of microcolony sizes, due to differences in their proliferation rates (Delgado-Ramos, 2016).

The first events that lead to these different proliferation patterns may come from small stochastic fluctuations in the expression profile, commonly designed as “noise”, that produces differences in proliferation (Newman et al., 2006; Pelechano et al., 2013) . If this fluctuation affects critical genes, as it has been described for the histone acetyltransferase *SIR2*, epigenetic changes can lead to stable expression patterns that provoke alteration in proliferation rates (Kyu Kang et al., n.d.; J. T. Smith et al., 2018; Song et al., 2014).

Epigenetic changes are frequently connected to aging and senescence. It has been demonstrated that old *S. cerevisiae* mother cells progressively lose proliferative capacity until they reach senescence (Campisi & D’Adda Di Fagagna, 2007). Replicative life span (the number of divisions that cells can make

before entering senescence (Campisi & D'Adda Di Fagagna, 2007; Michael Breitenbach et al., 2012; Mirisola & Longo, 2022) is longer than 20. The aging process of mother cells is characterized by accumulation of oxidative reactive species (ROS), increased cell volume and in the latest states of aging, increased DNA damage, loss of DNA repair capacity and failure to activate cell cycle checkpoints (Fehrmann et al., 2013; Hao et al., 2019; Yi et al., 2018). Very old cells are also deficient in the mechanism of asymmetric partitioning between mother and daughter cells, which prevents extrachromosomal rDNA circles and other aging factors to reach the latter (Hull & Houseley, 2020; Morlot et al., 2019; Sinclair & Guarente, 1997; Yang et al., 2015). The combination of these aging phenotypes contributes to increased generation time, provoking proliferative heterogeneity (Kamei et al., 2014; Knorre et al., 2018; Vaiserman et al., 2017; Wang et al., 2017; Xu & Teixeira, 2019) and ultimately lead to cell senescence and death (Frenk & Houseley, 2018; J. Smith et al., 2015).

In previous works, we performed transcriptomic analyses of yeast microcolonies according to their size, which revealed differential gene expression profiles between fast- and slow-growing clonal subpopulations (Delgado-Ramos, 2016). Among the most expressed genes in small microcolonies, we found the G1-S transition regulator Whi5[17], which represses expression of G1 cyclins by inhibiting the transcription factors SBF and MBF (De Bruin et al., 2004; Johnson & Skotheim, 2013; Wagner et al., 2009), in a similar manner to how Retinoblastoma protein controls G1-S transition in mammalian cells (Cooper, 2006; Michael Costanzo et al., 2004). It has been proposed that Whi5 levels acquired by daughter cells during budding is essential for size-dependent entry into G1 (Schmoller et al., 2015a). It has been also described that Whi5 accumulates in old aged cells, causing cell cycle delays and genomic instability that ultimately result in senescence and cell death (Neurohr et al., 2018).

These results led us to explore whether growth rates of microcolonies might be influenced by founder cell age, and whether variation of Whi5 levels might contribute to proliferation heterogeneity of populations that are genetically identical but intrinsically diverse in age. To answer these questions, we combined single cell microencapsulation with confocal microscopy and found that slow-

growing microcolonies are frequently founded by mother cells with a short number of divisions cycles, instead of the most abundant new-born cells. We also found that this reduction in the proliferation capacity of microcolonies founded by young mother cells is related to the expression levels of Whi5, which increases with mother cell age since the very first division. Our results establish that mother cell age can limit growth rates since early stages of yeast cells lifespan, and point to Whi5 level as a key element to understand proliferation heterogeneity

Results

A new method to analyze the replicative age of cells within a yeast microcolony

We have already shown that encapsulated microcolonies can be handled like particles suspended in a fluid, allowing, for example, their analysis in a large particle flow cytometer (García-Martínez et al., 2016). We conceived that it would also enable to perform the 3D analysis of individual microcolonies by confocal microscopy. We wondered whether such 3D analysis would help us to explain why some cells generate microcolonies at a lower proliferation rate than others.

We first established the criteria to microscopically detect those microcolonies with the most reduced proliferative rate. As described in Supplementary figure 1A, we considered “small” microcolonies (S) those with a diameter lower than 25 µm after encapsulation and 13 hours of incubation in optimal conditions. We considered “big” (B) colonies those larger than 50 µm in diameter, and “medium” (M) those in between 25 and 50 µm in diameter. As it is shown in Supplementary figure 1B, less than 30% of the microcolonies generated corresponded to the small category, presenting low proliferative capacity; more than 50% showed the size criteria to be defined as medium, and less than 20% were big ones.

In order to get insight on the genealogical structure of the microcolonies is important to know the replicative age of their cells. The number of bud scars is a perfect marker of replicative age. We proved that bud scars of encapsulated cells can be optimally detected after calcofluor staining, without affecting microcolony integrity as is shown in Supplementary figure 2.

After calcofluor staining, small microcolonies were analyzed under a confocal microscope. For each single small microcolony, we counted the total number of cells, as well as the number of bud scars present in each cell going through all Z axis images. We collected this data for more than 100 small microcolonies and analyzed the distribution of bud scars per cell in order to infer a genealogic pattern (supplementary table S1 and supplementary data: all images used in this study can be found at http://www.ebi.ac.uk/biostudies/ with the accession number S-BSST1071). As a quality control, we calculated the total number of bud scars (n) and checked whether it was compatible with the total number of cells counted (N). The number of scars should be always higher than the number of cells minus two ($n > N-2$). All microcolonies that did not fulfill this condition, likely founded by aggregated cells, were discarded.

In most cases, the distribution was consistent with the classical exponential growth. In this case unbudded newborn cells were the most frequent category, but never above 50%. This type of microcolonies also contained decreasing proportions of cells with one bud or more. The cell with the highest number of buds was identified as the likely founder of the colony. We refer to this category as the one that presents an “isotropic” growth pattern. The confocal analysis of a representative example of an isotropic small microcolony is presented in Figure 1A. In this example, the small microcolony is composed by 8 cells, indicating that after microencapsulation of a single cell, 7 divisions took place. The cell exhibiting 5 bud scars was identified as the founder. Four cells were newborns with no bud scars, and the other 3 cells showed an intermediate number of bud scars, indicating that they had divided during the development of the microcolony. The representation of a potential sequence of division events that explain the distribution of scars is shown in Figure 1B. Under this isotropic pattern, although the proliferation rate was low and only produced 8 cells in 13 h, no particular cell in the microcolony showed a stronger restriction to divide.

A second growth pattern was also detected in some small microcolonies. In this case the founder cell underwent division several times, but its daughter cells did not, or showed severe restrictions to do it. We refer to this category as the one that presents “anisotropic” growth. The confocal analysis of a representative

example of an anisotropic small microcolony is presented in Figure 1C. In this example the small microcolony presented 5 cells, indicating that 4 divisions took place after encapsulation of a single cell. The cell exhibiting 4 bud scars was identified as the founder. Three cells were newborns with no bud scars, and there was only one single-budded additional cell. This distribution of bud scars per cell, indicates that all but one these divisions were undergone by the founder. The representation of a potential sequence of division events that explain the anisotropic development of this microcolony is shown in Figure 1D.

Once we defined these two growth patterns, we quantified how many of the small microcolonies analyzed corresponded to each of them. We observed that most of them (83 out of 93) presented an isotropic growth pattern, while only 10 exhibited the anisotropic one (Table 1, Supplementary Table 1 and Supplementary images at http://www.ebi.ac.uk/biostudies/).

Small microcolonies are frequently founded by non-newborn cells.

To address whether replicative age contributes to the proliferation heterogeneity shown by clonal cells, we decided to identify the founder cell in each small microcolony and to estimate its replicative age at the time of foundation. As mentioned above, by counting the number of bud scars in all cells that compose a microcolony, it is possible to identify the founder cell. In order to estimate its replicative age at the encapsulation moment (A), we reasoned that the replicative age of the founder cell at the time of encapsulation must fit with the difference between the total number of bud scars in the microcolony (n) and the total number of cells (N) plus one. ($A = n - N + 1$) (see Materials and Methods).

In the example of Figure 1A-B, the 8 cells of the microcolony exhibited 11 bud scars in total, which indicated that the founder cell had divided already three times before funding the microcolony. In the second example (Figure 1C-D) the 5 cells showed 4 bud scars, which indicated that the founder cell was a newborn. Using this simple calculation, we were able to estimate the replicative age of the founder cells of the 93 small microcolonies analyzed (Supplementary Table 1). According to our analysis, most small microcolonies were founded by non-newborn cells.

This result was observed in both isotropic (more than a half) and anisotropic (nine out of ten) microcolonies (Table 1).

To really understand the relevance of this proportion of non-newborn cells as small microcolonies founders, we compared the age distribution of the founder cells (at the time of microencapsulation) to that of cells in an exponential liquid culture. As previously described (S. S. Lee et al., 2012a), most of the cells in the exponential culture were newborns (about 64%). Decreasing proportions of cells containing from 1 to 3 and more bud scars were also detected (Figure 2A in grey). Since we used exponential liquid cultures for cell microencapsulation, we would expect the same age distribution in the founder cells of small microcolonies. In contrast, the age distribution of small microcolonies founder cells (in red) was significantly different (*p value* below 0.000036) (Figure 2A): much fewer newborn founders than in the liquid culture, and higher frequency of founders that had undergone some divisions before encapsulation than expected (Figure 2A and Supplementary figure 3).

We also studied more in detail the size of these small microcolonies in relationship with the age of the founder cell. We found that most small microcolonies founded by newborns consisted of more than 16 cells, whereas most of those founded by mothers with three or more previous divisions exhibited less than 16 cells (Figure 2B). Small microcolonies founded by young mothers (one or two previous divisions) showed an intermediate size distribution (Figure 2B). These results indicate that a slight increase in the founder cell age is concomitant with a decrease in the proliferation rate of the microcolony.

The fact that microcolonies founded by rather young mother cells exhibited a higher probability of slow proliferate at a low rate argues for a negative influence of replicative age on cell proliferation since the earliest lifespan stages. In order to confirm this first conclusion of our study, we took advantage of the “Mother Enrichment Program” (MEP), an inducible genetic system, regulated by the presence of estradiol, which restricts the replicative capacity of daughter cells while allowing mother cells to achieve a normal replicative lifespan (Supplementary figure 4A) (Lindstrom & Gottschling, 2009). In the absence of

estradiol, mother and daughter cells can divide normally. However, in the presence of estradiol, daughter cells become unviable and the population enriches in mother cells of increasing age.

We hypothesized that a slightly aged population, not dominated by newborns but by mother cells that had already undergone one or two divisions, would increase the proportion of slow proliferating microcolonies after encapsulation. We first optimized the estradiol treatment required by the MEP strain DNY51 to undergo the very mild aging effect that we needed. We found that 3 h of incubation with estradiol was optimal to set a population with half of the newborns shown by the control culture and significant enrichment in mother cells with one or two bud scars (Supplementary figure 4B). While in the untreated population more than 60% of the cells were newborn, in the estradiol-treated culture 60% of the cells had budded once at least (Supplementary figure 4B).

These two cell populations were encapsulated and incubated for additional 13 hours in the absence of estradiol, to allow microcolonies formation without additional selection against daughter cells. Then, microcolonies were classified according to their size, as described in Supplementary figure 1A, and compared (Figure 2C). We found that the proportion of small microcolonies increased in the particles seeded with estradiol-treated cells as compared to the control samples, being the predominant microcolony category in this condition. The overall distribution of microcolony size was significantly altered by the very mild aging undergone by the founder cells (Square Chi test $p< 0,001$). This result strengthened the link between replicative age and proliferation rate, already in the very first stages of a mother cell lifespan, indicating that, once a daughter cell divides, there is a significant probability of its descending lineage to stably slow down its proliferation rate across generations.

Whi5 levels set proliferation rate during microcolony development.

As mentioned in the Introduction, after a transcriptomic analysis we had found that slow- and fast-proliferating microcolonies exhibited differential transcriptomic signatures. Specifically, *WHI5* was the most overexpressed gene in small

microcolonies (García-Martínez et al., 2016). In budding yeast, Whi5 is a G1/S transition inhibitor (Michael Costanzo et al., 2004) that contributes to both, the determination of critical cell size at START and cell fate (Litsios et al., 2022; Palumbo et al., 2016; Schmoller et al., 2015b, 2022). We decided to confirm that this correlation between Whi5 high levels and slow-proliferating (small) microcolonies was causative, in the sense that Whi5 levels determined slow proliferation and not vice versa. To do that, we used the *S. cerevisiae* KSY098 strain (Kukhtevich et al., 2020), where *WHI5* gene expression is under the regulation of chimeric regulator containing an estrogen-binding domain and responds to estradiol in a dose-dependent manner (Ottoz et al., 2014) (Figure 3A).

First, as shown in Figure 3B, we compared the microcolonies produced by encapsulated KSY098 cells, cultured in the absence of estradiol (referred as control in the B panel) and, therefore, expressing undetectable levels of Whi5 (Figure 3A), to those produced by isogenic W303 cells, which express *WHI5* from its own promoter. Lack of Whi5 expression produced a significant shift of the microcolony distribution towards the big category at the expense of medium and small ones (Figure 3B). This result confirmed that Whi5 plays a role in the proliferation heterogeneity detected in our microcolony assay and its expression is detrimental for the fast-growing subpopulation.

This result prompted us to hypothesize that, on the contrary, higher levels of Whi5 should favor slow-proliferating microcolonies. To test this hypothesis, we encapsulated exponentially growing KSY098 cells, in the absence of estradiol (not expressing *WHI5*). Single-cell seeded particles were then incubated without estradiol or in the presence of estradiol concentrations ranging between 2 and 10 nM (see Supplementary figure 5 for a synopsis of the experiment). Interestingly, cells incubated after encapsulation with 4nM estradiol showed a significant change in the microcolony distribution towards the small category, at the expense of the big one (Figure 3C). Higher concentrations of estradiol, which produced stronger expression of Whi5 (Figure 3A), also caused higher frequencies of small microcolonies (Figure 3C).

The proportion of cells expressing high Whi5 levels increases with age.

The results described above confirmed that small microcolonies associates with high Whi5 levels. We have also showed in this work that such small or slow-proliferating microcolonies were frequently founded by cells that had undergone more than one previous division cycle. We wondered whether these two phenomena were linked, in a way that Whi5 levels increase with replicative age.

To test this hypothesis, we analyzed cells expressing a Whi5-GFP fusion as the sole source of Whi5, and controlled by the endogenous *WHI5* promoter. Exponentially growing Whi5-GFP cells were sorted and collected according to their GFP signal, as described in detail in Material and Methods (see Supplementary figure 6 A and B for a synopsis of the experiment). We collected three different type of samples: i) cells with the highest Whi5-GFP expression (represented in green); ii) cells with the lowest Whi5-GFP expression (represented in purple); iii) a random sample of the whole population as a control (represented in blue) (Figure 4A). After that, each sample was stained with calcofluor and analyzed under the microscope to obtain the replicative age distribution of cells. We found the expected distribution of bud scar counts in the control sample, the random sample of the whole population (compare blue bars in Figure 4A). In contrast, when we analyze the distribution of bud scars in the sample with low Whi5-GFP levels a significant enrichment in newborn cells was observed (purple bars in Figure 4A). Moreover, the replicative age distribution of cells sorted for high Whi5-GFP levels presented a very clear reduction in newborn cells and an enrichment in cells with two or more division cycles (green bars in Figure 4A).

To analyze more in detail these results, in Figure 4B we represent, for each replicative age category, the ratio of number of cells with higher Whi5 levels (green) versus the total in this category.

Considered altogether, these results show that cells increase Whi5 expression as they undergo division cycles since very early stages. Thus, we conclude that Whi5 levels connects replicative age and proliferation rate since very early lifespan stages.

Discussion

Proliferative heterogeneity is coupled to replicative age since very early stages.

Heterogeneity in clonal populations can take many shapes, including proliferation rate (Knorre et al., 2018). We have focused on proliferative heterogeneity as we previously described that microencapsulated isogenic single cells produced microcolonies with a wide rank of sizes (García-Martínez et al., 2016). This heterogeneity in size is due to a difference in the number of cells that form the microcolony and, therefore, to a difference in the number of divisions carried out during the formation of the microcolony. In this work we tried to get insights on the basis of this proliferative heterogeneity studying the causes underlying slow proliferation in a controlled system of microcolonies.

To understand proliferative heterogeneity, studies cannot be performed in culture populations but analyzing individual cells and colonies. We have developed a direct and powerful methodology to analyze the generation of individual microcolonies from a single founder cell. We took advantage of our single cell encapsulation technique in combination with the analysis of individual microcolonies under confocal microscope. *In situ* calcofluor staining of bud scars in the whole encapsulated microcolony enabled us to establish the number of divisions performed by each cell. As is shown in the Results section (Figures 1, Table 1, Supplementary table 1, and Supplementary images at http://www.ebi.ac.uk/biostudies/) after counting (i) the total number of cells of an individual small microcolony, (ii) its total number of bud scars, and (iii) the number of bud scars of each cell within the microcolony, we were able to estimate the genealogy of such microcolony from its founder cell.

The first conclusion obtained using this technique, is that two different types of growth patterns can produce microcolonies with low proliferation rates. In the most frequent one (83 out of 93 small microcolonies analyzed), that we called “isotropic” growth, all cells participate in the low proliferation rate and no particular cell in the microcolony showed a stronger restriction to divide. The second small microcolony generation pattern, that we called “anisotropic” growth, is less

frequent (10 out of 93 small microcolonies analyzed) and involves that, while the founder cell undergoes division several times, its daughter cells do not, or show severe restrictions to do it. The distinction between these two different growth patterns driving slow proliferation is an example of the utility of the method that we describe in this work

Our analyses also provide relevant information on the age of founder cells at the moment of encapsulation, that is, when the studies microcolonies were initiated. According to our analyses, most slow-proliferating microcolonies were founded by non-newborn cells, both in isotropic and anisotropic types. While the liquid cultures used for encapsulation presented the well-known distribution of cell ages of exponentially growing populations (Keinan et al., 2018; S. S. Lee et al., 2012b; Lord & Wheals, 1980) characterized by a majority of newborn cells without bud scars (64%) followed by progressively reducing subpopulations of cells with 1, 2, 3 and more bud scars (Figure 2A), slow-proliferating microcolonies founder cells did not fit this proportion. In fact, they were enriched in cells that had performed one or more divisions before encapsulation (Figure 2A). Moreover, the smaller the microcolony, the higher proportion of older founder cells (Figure 2B). Finally, using the MEP system to enrich in non-newborn founder cells (1 or 2 divisions old) we got a significant increase in slow-proliferating microcolonies (Figure 2C). We conclude that once a newborn cell divides, there is a significant probability of its descending lineage to stably slow down its proliferation rate across generations. In other words: the restriction in proliferation capacity imposed by replicative age can be established in any stage of the mother cell lifespan, even during its first division.

It is important to emphasize that the impact in proliferation rate that we describe takes place at the very early stages of the replicative lifespan, since this connection has been so far studied from the perspective of the last divisions (after more than 10 replicative cycles) that a mother cell undergoes before death (Egilmez & Jazwinski, 1989; S. Michal Jazwinski, 1999; J. Smith et al., 2015). Secondly, the impact on proliferation rate from the very first divisions gives better understanding on the proliferative heterogeneity observed in exponential cultures, where proportion of older cells (more than 10 divisions) are quite insignificant (García-Martínez et al., 2016). Finally, our data support the idea that

changes in young mother cells proliferation capacity have a much greater impact on population fitness than does functional deterioration at later ages and may play a substantial role in adaptations to changing environments (Knorre et al., 2018).

Whi5 levels link proliferative heterogeneity to replicative age since early stages

Cell cycle progression requires complex regulatory networks in eukaryotic cells to ensure functional success (Delgado-Román & Muñoz-Centeno, 2021). Timing of Start at late G1 is regulated by the antagonic interplay between the Cln3 G1 cyclin and the Whi5 inhibitor (De Bruin et al., 2004). Increased synthesis of Cln3 and dilution of Whi5 levels due to cell size increase has been proposed to control has also been proposed to control Start timing and cell size-dependent proliferation (Litsios et al., 2022) (Schmoller et al., 2015b). As cell size increases, Whi5 protein would be progressively diluted and, once it has reached a certain threshold concentration, which should correspond to an optimal division size, cells commit to division (Schmoller et al., 2015b). In this work we found a strong connection between Whi5 levels and proliferation heterogeneity. By modulating Whi5 levels, we showed a direct correlation between Whi5 levels and the proportion of slow-proliferating microcolonies (Figure 3A-C). Furthermore, sorting experiments shown in Figure 4, using a budding yeast strain containing a Whi5-GFP version, demonstrate that at higher replicative ages, high Whi5 levels are more frequent. This result confirmed our previously published finding that smallest microcolonies, mostly founded by non-newborn cells, overexpressed Whi5 (García-Martínez et al., 2016).

It has been described that Whi5 accumulates in old aged cells, causing cell cycle delays and genomic instability that ultimately result in cell death (Neurohr et al., 2018). However, this description was based on mother cells after more than 10 division cycles, closed to the end of its life span. Our results demonstrate that accumulation of Whi5 can start happening at any division of a mother cell, since very early stages, and allow proposing Whi5 as the key regulator of proliferation heterogeneity across generations in budding yeast populations.

The combination of our results is compatible with a model (Supplementary figure 7) in which a newborn cell with optimal proliferation capacity can undergo an increase in Whi5 expression at any division cycle, since the very first. This increased in Whi5 levels would negatively condition the proliferation rate of its progeny, favoring extensive growth heterogeneity of the whole population. Increase of Whi5 might be due to stochastic noise in its expression, but might also be linked to its time of expression during the cell cycle, which seems to be maximal in G2/M (Granovskaia et al., 2010). Any delay in G2/M, due for instance to activation of checkpoint mechanisms, might provoke increased Whi5 levels, which in turn would induce subsequent cell-cycle alterations, enabling a self-regulatory loop that propagates throughout the cell linage. Such activation of checkpoints has been described to play a role in mitotic catastrophe during late aging (Crane et al., 2019). Our work suggest that it may be a more common phenomenon, potentially being triggered in any stage of replicative life span, and explaining the high proliferative heterogeneity of cell populations.

Materials and Methods

Strains

The wildtype BY4741 strain was obtained from the EUROSCARF yeast collection. Whi5 tagged with GFP was obtained from Thermo Fisher Scientific GFP yeast clone collection. See supplementary table 2 for a list of all strains used in this work.

Name	**Genotype**	**Source**
BY4741	*MATa; his3Δ1; leu2Δ0; met15Δ0; ura3Δ0*	Euroscarf
DNY51	*Mat a can1::PSTE2-Sp_his5 leu2Δyp1Δ met15Δ hoΔ::PSCWII-cre-EBD78-NATMX loxP-ubc9-LOXp-Leu2 loxP-CDC20-Intron-loxP-HPHMX*	From Lindstrom & Gottschling, 2009

KSY098-1	*Mat a; his3::LexA-ER-AD-TF-HIS3 whi5::kanMX6-LexApr-Whi5-mCherry-Adh1term-Leu2*	From Kukhtevich et al., 2020
W303	*Mat a leu2Δ3 112 trp1-1 can1-100 ura3Δ1 ade2Δ1 his3Δ11 15*	Lab collection
Whi5GFP	*Mat a his3Δ1 leu2Δ0 met15Δ0 ura3Δ0 Whi5-GFP::HIS3*	Thermo Fisher Scientific GFP yeast clone collection

Microencapsulation

Microencapsulation conditions were set to obtain single cell capsules to ensure that all the cells growing inside every capsule were clonal. First, cells were cultured to a O.D of approximately 0.5 to ensure that it was at exponential growth phase. Microencapsulation of individual yeast cells in alginate microparticles was performed using a Cellena microencapsulator (Ingeniatrics) following a well described protocol already published (Delgado-Ramos, 2016; García-Martínez et al., 2016). After the microencapsulation, capsules are collected and cultured together in YPD for 13 hours at 30ºC continuous stirring.

Mother cell enrichment

DNY51 cells were grown at normal culture conditions to exponential phase, they were then collected and inoculated in 10ml of YPD (previously preheated at 30ºC) and estradiol at a final 1μM concentration. They were cultured at 30ºC for 3 hours. The estradiol was then washed, and cells were resuspended in YPD to finally add them to the microencapsulation mixture. After the microencapsulation, capsules were collected and cultured in YPD (without estradiol) for 13 hours at 30 ºC. DNY51 strain was used for liquid aging assays. It was previously described in (Lindstrom & Gottschling, 2009). This strain presents a construction which allows

a selection against newborn daughter cells through a “mother enrichment program” or “MEP”. Cre-EBD78, a novel version of a fusion protein between the Cre recombinase from bacteriophage P1 and the estrogen-binding domain of the murine estrogen receptor that is strictly dependent on β-estradiol for activity. PSCW11-cre-EBD78 is integrated at the ho locus and specifically expressed in newborn cells, using a daughter-specific promoter derived from SCW11. Target genes were constructed at their endogenous loci by introduction of loxP sites. Target genes are UBC9 and CDC20, both necessary elements for cell cycle progression. In β-estradiol treatment conditions, Cre recombinase translocates to the nucleus and, as a consequence of its activity, target genes are removed only in newborn cells, as PSCW11-cre-EBD78 expression is restricted to those

Modulation of Whi5 expression

KSY098-1 strain, kindly provided by Kurt Schmoller, is constructed by the addition of the chimeric protein LexA-ER-AD. Lex A is a DNA binding protein, ER is the human receptor for Estrogen, which strongly responds to β-estradiol. AD is an activation domain. In the absence of β-estradiol, whi5 expression inactivated but, in the presence of this hormone, the AD is activated, which leads to the activation of Whi5 expression (Kukhtevich et al., 2020). A KSY089-1 culture was first growth to exponential phase (D.O.=0.5) and then microencapsulated following the usual protocol of microencapsulation. After that, microcapsules, which have one single cell trapped each, were collected and then inoculated in flasks with YPD and estradiol at different concentrations: one flask with no estradiol for the control, the others with 2nM, 4nM, 5nM, 6nM, 8nM and 10nM respectively. The wildtype W303 control was separately encapsulated the same day. Finally, these and the W303 wildtype strain were cultured for 9,5 hours at 30 degrees.

Light microscopy and microcolony size analysis

Microcolony sizes analysis was performed using an optical microscope (Leica DM750). Microcolonies were classified according to their size in small, medium and big microcolonies. As capsule diameter is stable (approximately 100μm), big microcolonies are considered those that surpass the radio of the capsule, medium microcolonies are those whose size range between half the radio and

the radio, and the ones smaller than half the radio are considered small microcolonies (Supplementary Figure 1A).

Calcofluor staining

For replicative age analysis of a wildtype exponential culture, a bud scar staining was performed. First, cells were collected at exponential growth phase, fixated with 70% Ethanol and stored at 4ºC for at least 2 hours. After that, cells were washed with PBS 1X and resuspended in a solution of PBS and calcofluor (Fluorescent Brightener 28 (Sigma Aldrich)) at a final concentration of 0.1 mg/ml. They were incubated for 5 to 10 minutes in dark conditions at room temperature and then washed again with PBS. Cells were finally resuspended in 100μl of PBS. Microcolonies were also stained with calcofluor for small microcolonies founder cell identification. First, fixated microcolonies (YPD and Ethanol 70% 1:1) were filtrated and collected. They were washed with a TrisHCl-CaCl 2:1 solution and inoculated in 0.5ml of calcofluor at 0.1 mg/ml concentration for 5 minutes at room temperature. After that, microcapsules were filtrated and washed again with TrisHCl-CaCl solution. Finally, they were collected and preserved in 0.5ml of the same solution.

Fluorescent microscopy and bud scar counting

Replicative age of the population was calculated by manually counting the number of cells bud scars using a direct fluorescent microscope Olympus BX-61. Bud scars were detectable using the DAPI filter. Cells were classified according to the number of bud scars, which is a direct method to know their replicative age.

Confocal microscopy and founder cells age analysis

Microcolonies stained with calcofluor were visualized in a A1R Confocal Nikon Microscope using the 60X oil objective and DAPI filter. Images of small microcolonies (n=187) were taken every 0.5 μM in Z-axis. Total number of cells and total number of bud scars were counted going through all Z axis images. Using the formula $number\ of\ budscars - number\ of\ cells + 1 = founder\ cell\ age$ the replicative age of the small microcolonies founder cells at

initial time (right before founding the small microcolony) was estimated. The resulting number was corrected when incoherent: very high numbers usually meant that the small microcolony was founded by two aged cells. These cases were taken out of the analysis. On the other hand, negative numbers probably meant that the number of bud scars was underestimated. Going through the genealogy of the small microcolonies, taken into consideration the number of buds observed on each cell, these numbers were corrected according to the most probable scenario (being usually the case of a virgin cell founder).

Whi5GFP Cell sorting

Whi5-GFP strain was cultured to exponential growth phase in minimum media complemented with all the essential amino acids except Histidine. Then, cells were collected at DO_{600nm} 0.5 and sorted in a BD FACSJazz™ cell sorter according to the GFP intensity detected. Cells with low Whi5 expression sorting criteria was stablished according to a negative (not fluorescent) control BY4741. Cells with higher Whi5 expression were selected drawing the sorting gate for the 5% of cells with highest Whi5 GFP expression. After sorting, each sample was stained with calcofluor and analyzed.

References

Ackermann, M. (2015). A functional perspective on phenotypic heterogeneity in microorganisms. In *Nature Reviews Microbiology* (Vol. 13, Issue 8, pp. 497–508). Nature Publishing Group. https://doi.org/10.1038/nrmicro3491

Campisi, J., & D'Adda Di Fagagna, F. (2007). Cellular senescence: When bad things happen to good cells. In *Nature Reviews Molecular Cell Biology* (Vol. 8, Issue 9, pp. 729–740). https://doi.org/10.1038/nrm2233

Cooper, K. (2006). Rb, whi it's not just for metazoans anymore. In *Oncogene* (Vol. 25, Issue 38, pp. 5228–5232). https://doi.org/10.1038/sj.onc.1209630

Cota, I., Blanc-Potard, A. B., & Casadesús, J. (2012). STM2209-STM2208 (opvAB): A phase variation locus of salmonella enterica involved in control of O-antigen chain length. *PLoS ONE*, *7*(5). https://doi.org/10.1371/journal.pone.0036863

Crane, M. M., Tsuchiya, M., Blue, B. W., Almazan, J. D., Chen, K. L., Duffy, S. R., Golubeva, A., Grimm, A. M., Guard, A. M., Hill, S. A., Huynh, E., Kelly, R. M., Kiflezghi, M., Kim, H. D., Lee, M., Lee, T. I., Li, J., Nguyen, B. M. G., Whalen, R. M., … Kaeberlein, M. (2019). Rb analog Whi5 regulates G1 to S transition and cell size but not replicative lifespan in budding yeast. *Translational Medicine of Aging*, *3*, 104–108. https://doi.org/10.1016/j.tma.2019.10.002

Davis, K. M., & Isberg, R. R. (2016). Defining heterogeneity within bacterial populations via single cell approaches. In *BioEssays* (Vol. 38, Issue 8, pp. 782–790). John Wiley and Sons Inc. https://doi.org/10.1002/bies.201500121

De Bruin, R. A. M., Mcdonald, W. H., Kalashnikova, T. I., Yates, J., & Wittenberg, C. (2004). Cln3 Activates G1-Specific Transcription via Phosphorylation of the SBF Bound Repressor Whi5 fall into the G1-specific gene family (Cho et al they govern the events associated with cell cycle initiation, including DNA repli. In *Cell* (Vol. 117). Together.

Delgado-Ramos, L. (2016). *Microbial analysis by microencapsulation and its application to study proliferation heterogeneity*. Universidad de Sevilla.

Delgado-Román, I., & Muñoz-Centeno, M. C. (2021). Coupling Between Cell Cycle Progression and the Nuclear RNA Polymerases System. In *Frontiers in Molecular Biosciences* (Vol. 8). Frontiers Media S.A. https://doi.org/10.3389/fmolb.2021.691636

Egilmez, N. K., & Jazwinski, S. M. (1989). Evidence for the Involvement of a Cytoplasmic Factor in the Aging of the Yeast Saccharomyces cerevisiae. In *JOURNAL OF BACTERIOLOGY* (Vol. 171, Issue 1).

Fehrmann, S., Paoletti, C., Goulev, Y., Ungureanu, A., Aguilaniu, H., & Charvin, G. (2013). Aging yeast cells undergo a sharp entry into senescence unrelated to the loss of mitochondrial membrane potential. *Cell Reports*, *5*(6), 1589–1599. https://doi.org/10.1016/j.celrep.2013.11.013

Frenk, S., & Houseley, J. (2018). Gene expression hallmarks of cellular ageing. *Biogerontology*, *19*(6), 547–566. https://doi.org/10.1007/s10522-018-9750-z

García-Martínez, J., Delgado-Ramos, L., Ayala, G., Pelechano, V., Medina, D. A., Carrasco, F., González, R., Andrés-León, E., Steinmetz, L., Warringer, J., Chávez, S., & Pérez-Ortín, J. E. (2016). The cellular growth rate controls overall mRNA turnover, and modulates either transcription or degradation rates of particular gene regulons. *Nucleic Acids Research*, *44*(8), 3643–3658. https://doi.org/10.1093/nar/gkv1512

Ghosh, D., Veeraraghavan, B., Elangovan, R., & Vivekanandan, P. (2020). Antibiotic resistance and epigenetics: More to it than meets the eye. *Antimicrobial Agents and Chemotherapy*, *64*(2). https://doi.org/10.1128/AAC.02225-19

Granovskaia, M. V., Jensen, L. J., Ritchie, M. E., Toedling, J., Ning, Y., Bork, P., Huber, W., & Steinmetz, L. M. (2010). High-resolution transcription atlas of the mitotic cell cycle in budding yeast. *Genome Biology*, *11*(3). https://doi.org/10.1186/gb-2010-11-3-r24

Hao, N., Crane, M. M., Russell, A. E., Schafer, B. J., Blue, B. W., Whalen, R., Almazan, J., Gi Hong, M., Nguyen, B., Goings, J. E., Chen, K. L., Kelly, R., & Kaeberlein, M. (2019). *DNA damage checkpoint activation impairs chromatin homeostasis and promotes mitotic catastrophe during aging*. https://doi.org/10.7554/eLife.50778.001

Hull, R. M., & Houseley, J. (2020). The adaptive potential of circular DNA accumulation in ageing cells. In *Current Genetics* (Vol. 66, Issue 5, pp. 889–894). Springer Science and Business Media Deutschland GmbH. https://doi.org/10.1007/s00294-020-01069-9

Johnson, A., & Skotheim, J. M. (2013). Start and the restriction point. In *Current Opinion in Cell Biology* (Vol. 25, Issue 6, pp. 717–723). https://doi.org/10.1016/j.ceb.2013.07.010

Kamei, Y., Tamada, Y., Nakayama, Y., Fukusaki, E., & Mukai, Y. (2014). Changes in transcription and metabolism during the early stage of replicative cellular senescence in budding yeast. *Journal of Biological Chemistry*, *289*(46), 32081–32093. https://doi.org/10.1074/jbc.M114.600528

Keinan, E., Abraham, A. C., Cohen, A., Alexandrov, A. I., Mintz, R., Cohen, M., Reichmann, D., Kaganovich, D., & Nahmias, Y. (2018). High-Reynolds Microfluidic Sorting of Large Yeast Populations. *Scientific Reports*, *8*(1). https://doi.org/10.1038/s41598-018-31726-6

Knorre, D. A., Azbarova, A. V., Galkina, K. V., Feniouk, B. A., & Severin, F. F. (2018). Replicative aging as a source of cell heterogeneity in budding yeast. In *Mechanisms of Ageing and Development* (Vol. 176, pp. 24–31). Elsevier Ireland Ltd. https://doi.org/10.1016/j.mad.2018.09.001

Kukhtevich, I. V., Lohrberg, N., Padovani, F., Schneider, R., & Schmoller, K. M. (2020). Cell size sets the diameter of the budding yeast contractile ring. *Nature Communications*, *11*(1). https://doi.org/10.1038/s41467-020-16764-x

Kyu Kang, W., Hyeock Kim, Y., Ah Kang, H., Kwon, K.-S., & Kim, J.-Y. (n.d.). *Sir2 phosphorylation through cAMP-PKA and CK2 signaling inhibits the lifespan extension activity of Sir2 in yeast*. https://doi.org/10.7554/eLife.09709.001

Lee, J. A., Riazi, S., Nemati, S., Bazurto, J. V., Vasdekis, A. E., Ridenhour, B. J., Remien, C. H., & Marx, C. J. (2019). Microbial phenotypic heterogeneity in response to a metabolic toxin: Continuous, dynamically shifting distribution of formaldehyde tolerance in Methylobacterium extorquens populations. *PLoS Genetics*, *15*(11). https://doi.org/10.1371/journal.pgen.1008458

Lee, S. S., Vizcarra, I. A., Huberts, D. H. E. W., Lee, L. P., & Heinemann, M. (2012a). Whole lifespan microscopic observation of budding yeast aging through a microfluidic dissection platform. *Proceedings of the National Academy of Sciences of the United States of America*, *109*(13), 4916–4920. https://doi.org/10.1073/pnas.1113505109

Lee, S. S., Vizcarra, I. A., Huberts, D. H. E. W., Lee, L. P., & Heinemann, M. (2012b). Whole lifespan microscopic observation of budding yeast aging through a microfluidic dissection platform. *Proceedings of the National Academy of Sciences of the United States of America*, *109*(13), 4916–4920. https://doi.org/10.1073/pnas.1113505109

Levy, S. F., Ziv, N., & Siegal, M. L. (2012). Bet hedging in yeast by heterogeneous, age-correlated expression of a stress protectant. *PLoS Biology*, *10*(5). https://doi.org/10.1371/journal.pbio.1001325

Lindstrom, D. L., & Gottschling, D. E. (2009). The mother enrichment program: A genetic system for facile replicative life span analysis in Saccharomyces cerevisiae. *Genetics*, *183*(2), 413–422. https://doi.org/10.1534/genetics.109.106229

Litsios, A., Goswami, P., Terpstra, H. M., Coffin, C., Vuillemenot, L. A., Rovetta, M., Ghazal, G., Guerra, P., Buczak, K., Schmidt, A., Tollis, S., Tyers, M., Royer, C. A., Milias-Argeitis, A., & Heinemann, M. (2022). The timing of Start is determined primarily by increased synthesis of the Cln3 activator rather than dilution of the Whi5 inhibitor. *Molecular Biology of the Cell*, *33*(5), rp2. https://doi.org/10.1091/mbc.E21-07-0349

Lord, P. G., & Wheals, A. E. (1980). Asymmetrical Division of Saccharomyces cerevisiae. In *JOURNAL OF BACTERIOLOGY* (Vol. 142, Issue 3).

Martins, B. M. C., & Locke, J. C. W. (2015). Microbial individuality: how single-cell heterogeneity enables population level strategies. In *Current Opinion in Microbiology* (Vol. 24, pp. 104–112). Elsevier Ltd. https://doi.org/10.1016/j.mib.2015.01.003

Michael Breitenbach, S. Michal Jazwinski, & Peter Laun. (2012). *Aging Research in Yeast* (Michael Breitenbach, S. Michal Jazwinski, & Peter Laun, Eds.; 1st ed., Vol. 57). Springer Dordrecht.

Michael Costanzo, Joy L Nishikawa, Xiaojing Tang, Jonathan S Millman, Oliver Schub, Kevin Breitkreuz, Danielle Dewar, Ivan Rupes, Brenda Andrews, & Mike Tyers. (2004). CDK Activity Antagonizes Whi5, an Inhibitor of G1/S Transcription in Yeast. *Cell*, *117*(7), 899–913. http://www.cell.com/

Mirisola, M. G., & Longo, V. D. (2022). Yeast Chronological Lifespan: Longevity Regulatory Genes and Mechanisms. In *Cells* (Vol. 11, Issue 10). MDPI. https://doi.org/10.3390/cells11101714

Morlot, S., Song, J., Léger-Silvestre, I., Matifas, A., Gadal, O., & Charvin, G. (2019). Excessive rDNA Transcription Drives the Disruption in Nuclear Homeostasis during Entry into Senescence in Budding Yeast. *Cell Reports*, *28*(2), 408-422.e4. https://doi.org/10.1016/j.celrep.2019.06.032

Neurohr, G. E., Terry, R. L., Sandikci, A., Zou, K., Li, H., & Amon, A. (2018). Deregulation of the G1/S-phase transition is the proximal cause of mortality in old yeast mother cells. *Genes and Development*, *32*(15–16), 1075–1084. https://doi.org/10.1101/gad.312140.118

Newman, J. R. S., Ghaemmaghami, S., Ihmels, J., Breslow, D. K., Noble, M., DeRisi, J. L., & Weissman, J. S. (2006). Single-cell proteomic analysis of S. cerevisiae reveals the architecture of biological noise. *Nature*, *441*(7095), 840–846. https://doi.org/10.1038/nature04785

Olivenza, D. R., Nicoloff, H., Antonia Sánchez-Romero, M., Cota, I., Andersson, D. I., & Casadesús, J. (2019). A portable epigenetic switch for bistable gene expression in bacteria. *Scientific Reports*, *9*(1). https://doi.org/10.1038/s41598-019-47650-2

Ottoz, D. S. M., Rudolf, F., & Stelling, J. (2014). Inducible, tightly regulated and growth condition-independent transcription factor in Saccharomyces cerevisiae. *Nucleic Acids Research*, *42*(17). https://doi.org/10.1093/nar/gku616

Palumbo, P., Vanoni, M., Cusimano, V., Busti, S., Marano, F., Manes, C., & Alberghina, L. (2016). Whi5 phosphorylation embedded in the G 1 /S network dynamically controls critical cell size and cell fate. *Nature Communications*, *7*. https://doi.org/10.1038/ncomms11372

Pelechano, V., Wei, W., & Steinmetz, L. M. (2013). Extensive transcriptional heterogeneity revealed by isoform profiling. *Nature*, *497*(7447), 127–131. https://doi.org/10.1038/nature12121

Ryall, B., Eydallin, G., & Ferenci, T. (2012). Culture History and Population Heterogeneity as Determinants of Bacterial Adaptation: the Adaptomics of a Single Environmental Transition. *Microbiology and Molecular Biology Reviews*, *76*(3), 597–625. https://doi.org/10.1128/mmbr.05028-11

S. Michal Jazwinski. (1999). Molecular mechanisms of yeast longevity. *Trends in Microbiology*, *7*(6), 247–252.

Sampaio, N. M. V., & Dunlop, M. J. (2020). Functional roles of microbial cell-to-cell heterogeneity and emerging technologies for analysis and control. In *Current Opinion in Microbiology* (Vol. 57, pp. 87–94). Elsevier Ltd. https://doi.org/10.1016/j.mib.2020.08.002

Sánchez-Romero, M. A., & Casadesús, J. (2014). Contribution of phenotypic heterogeneity to adaptive antibiotic resistance. *Proceedings of the National Academy of Sciences of the United States of America*, *111*(1), 355–360. https://doi.org/10.1073/pnas.1316084111

Schmoller, K. M., Lanz, M. C., Kim, J., Koivomagi, M., Qu, Y., Tang, C., Kukhtevich, I. V., Schneider, R., Rudolf, F., Moreno, D. F., Aldea, M., Lucena, R., & Skotheim, J. M. (2022). Whi5 is diluted and protein synthesis does not dramatically increase in pre-Start G1. *Molecular Biology of the Cell*, *33*(5), lt1. https://doi.org/10.1091/mbc.E21-01-0029

Schmoller, K. M., Turner, J. J., Kõivomägi, M., & Skotheim, J. M. (2015a). Dilution of the cell cycle inhibitor Whi5 controls budding-yeast cell size. *Nature*, *526*(7572), 268–272. https://doi.org/10.1038/nature14908

Schmoller, K. M., Turner, J. J., Kõivomägi, M., & Skotheim, J. M. (2015b). Dilution of the cell cycle inhibitor Whi5 controls budding-yeast cell size. *Nature*, *526*(7572), 268–272. https://doi.org/10.1038/nature14908

Sinclair, D. A., & Guarente, L. (1997). Extrachromosomal rDNA Circles-A Cause of Aging in Yeast. In *Cell* (Vol. 91).

Smith, J. T., White, J. W., Dungrawala, H., Hua, H., & Schneider, B. L. (2018). Yeast lifespan variation correlates with cell growth and sir2 expression. *PLoS ONE*, *13*(7). https://doi.org/10.1371/journal.pone.0200275

Smith, J., Wright, J., & Schneider, B. L. (2015). A budding yeast's perspective on aging: The shape I'm in. *Experimental Biology and Medicine*, *240*(6), 701–710. https://doi.org/10.1177/1535370215577584

Song, J., Yang, Q., Yang, J., Larsson, L., Hao, X., Zhu, X., Malmgren-Hill, S., Cvijovic, M., Fernandez-Rodriguez, J., Grantham, J., Gustafsson, C. M., Liu, B., & Nyström, T. (2014). Essential Genetic Interactors of SIR2 Required for Spatial Sequestration and Asymmetrical Inheritance of Protein Aggregates. *PLoS Genetics*, *10*(7). https://doi.org/10.1371/journal.pgen.1004539

Vaiserman, A. M., Koliada, A. K., & Jirtle, R. L. (2017). Non-genomic transmission of longevity between generations: Potential mechanisms and evidence across species. In *Epigenetics and Chromatin* (Vol. 10, Issue 1). BioMed Central Ltd. https://doi.org/10.1186/s13072-017-0145-1

Wagner, M. V., Smolka, M. B., de Bruin, R. A. M., Zhou, H., Wittenberg, C., & Dowdy, S. F. (2009). Whi5 regulation by site specific CDK-phosphorylation in Saccharomyces cerevisiae. *PLoS ONE*, *4*(1). https://doi.org/10.1371/journal.pone.0004300

Wang, Y., Lo, W. C., & Chou, C. S. (2017). A modeling study of budding yeast colony formation and its relationship to budding pattern and aging. *PLoS Computational Biology*, *13*(11). https://doi.org/10.1371/journal.pcbi.1005843

Xu, Z., & Teixeira, M. T. (2019). The many types of heterogeneity in replicative senescence. *Yeast*, *36*(11), 637–648. https://doi.org/10.1002/yea.3433

Yang, J., McCormick, M. A., Zheng, J., Xie, Z., Tsuchiya, M., Tsuchiyama, S., El-Samad, H., Ouyang, Q., Kaeberlein, M., Kennedy, B. K., & Li, H. (2015). Systematic analysis of asymmetric partitioning of yeast proteome between mother and daughter cells reveals 'aging factors'

and mechanism of lifespan asymmetry. *Proceedings of the National Academy of Sciences of the United States of America*, *112*(38), 11977–11982. https://doi.org/10.1073/pnas.1506054112

Yi, D. G., Hong, S., & Huh, W. K. (2018). Mitochondrial dysfunction reduces yeast replicative lifespan by elevating RAS-dependent ROS production by the ER-localized NADPH oxidase Yno1. *PLoS ONE*, *13*(6). https://doi.org/10.1371/journal.pone.0198619

Ziv, N., Siegal, M. L., & Gresham, D. (2013). Genetic and nongenetic determinants of cell growth variation assessed by high-throughput microscopy. *Molecular Biology and Evolution*, *30*(12), 2568–2578. https://doi.org/10.1093/molbev/mst138

A

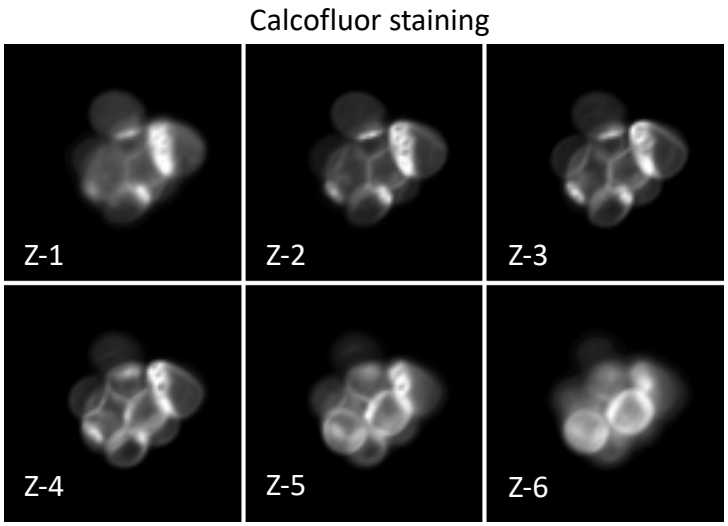
Calcofluor staining
Z-1
Z-2
Z-3
Z-4
Z-5
Z-6

B

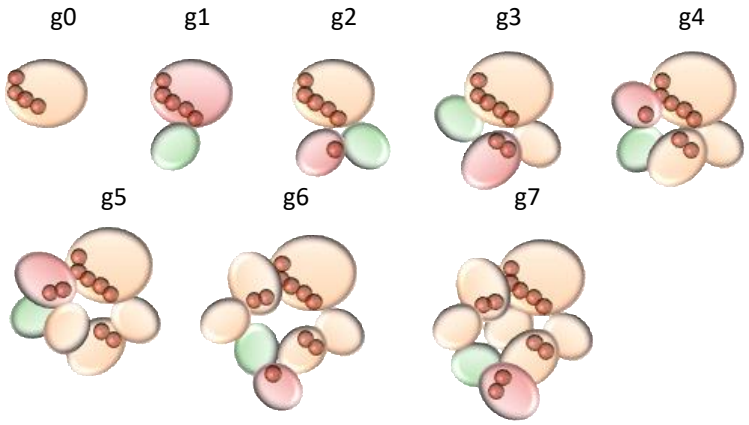
g0
g1
g2
g3
g4
g5
g6
g7

C

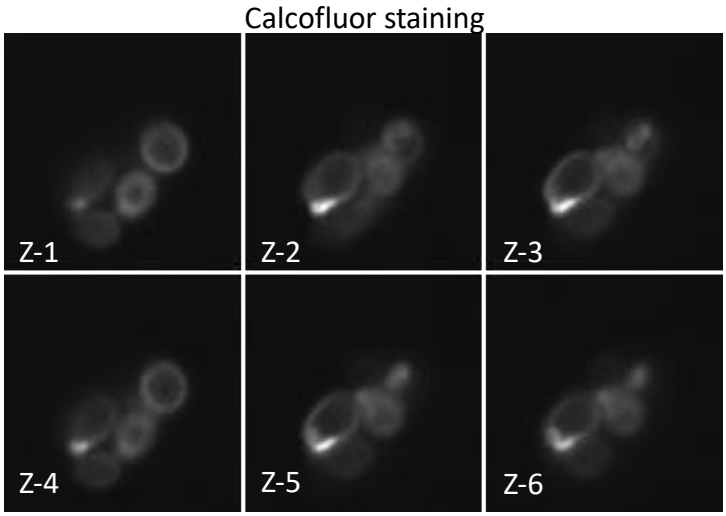
Calcofluor staining
Z-1
Z-2
Z-3
Z-4
Z-5
Z-6

D

g0
g1
g2
g3
g4

Figure 1. Examples of the two categories of small microcolonies found, differentiated by the division pattern of the cells within the microcolony. **(A)** Confocal image (Z stacks of the same small microcolony Z1-6) of a small microcolony taken at 13 hours after growth. This small microcolony founder cell was not virgin when it founded the microcolony at g0. (**B**) Graphical representation of the same small microcolony shown in (A), which presents an isotropic small microcolony genealogy pattern. In this category are included those whose cells divide equally. The header letters g0-g7 indicates the hypothetical time at which a new division occurs. For every division, the mother cell is coloured in red and the daughter new-born cell in green. (**C**) Confocal image of another small microcolony at 13 hours of growth. This small microcolony was founded by a virgin cell. (**D**) Genealogy of the microcolony shown in (C), which presents an anisotropic type of growth. In this category are included those whose founder cell or first-born cell are the only one dividing.

A

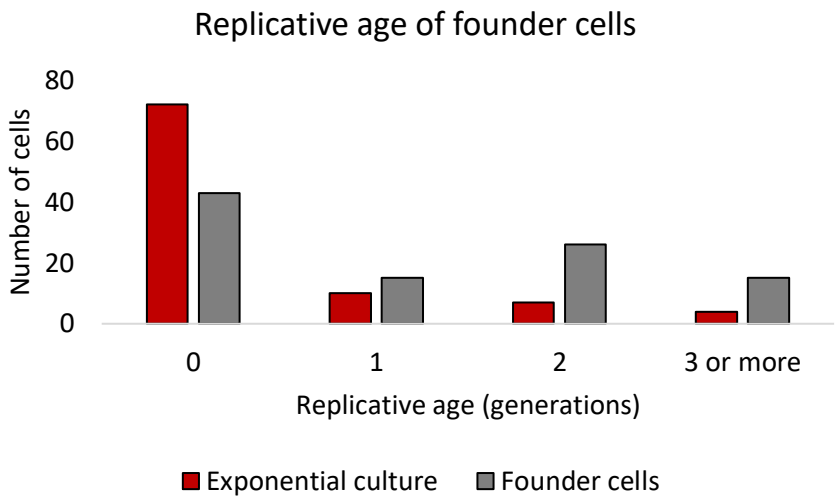
Replicative age of founder cells
Number of cells
80
60
40
20
0
0
1
2
3 or more
Replicative age (generations)
Exponential culture
Founder cells

B

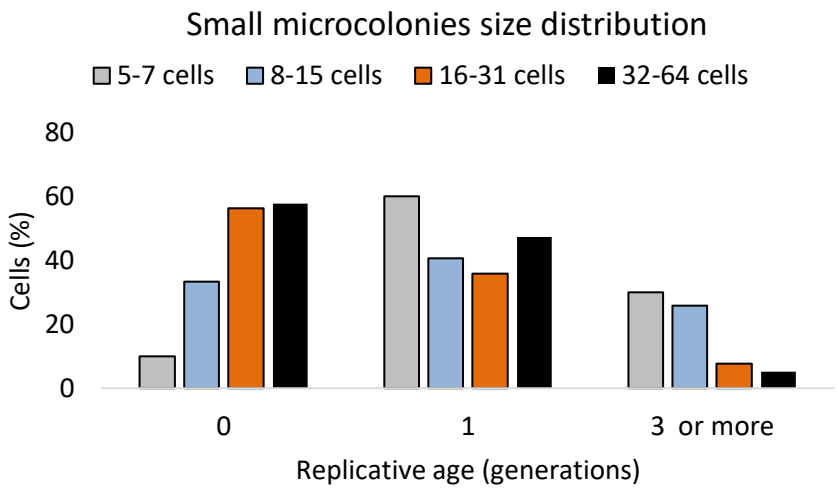
Small microcolonies size distribution
5-7 cells
8-15 cells
16-31 cells
32-64 cells
Cells (%)
80
60
40
20
0
0
1
3 or more
Replicative age (generations)

C

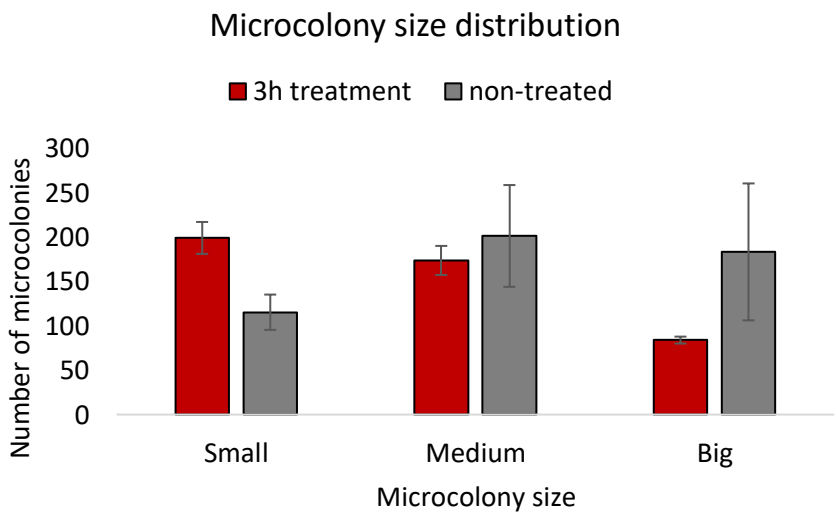
Microcolony size distribution
3h treatment
non-treated
Number of microcolonies
300
250
200
150
100
50
0
Small
Medium
Big
Microcolony size

Figure 2. Small microcolonies are frequently founded by cells with a replicative age greater than 0. **(A)** Distribution of small microcolonies founder cells (grey) according to their replicative age before founding the microcolony (n=96) compared to that of the initial exponential culture before encapsulating (red) (n=96). Small microcolonies are more frequently founded by cells with a replicative age greater than 0. The statistical test realized was a chi square test with a result of a *p value* equal to 3,6 * 10^{-6}. (**B)** Frequency of founder cells according to their replicative age that founded small microcolonies of different sizes. From bigger to smaller small microcolonies, we decided to group them into 4 categories: 32-64 cells, 16-31 cells, 8-15 cells and 5-7 cells. A progressively increase in the number of founder cell bud scars can be observed in smaller categories. **(C)** Distribution of microcolonies according to their size (small, medium or big) in a wildtype non-aged culture (no estradiol, in grey) and in a wildtype aged culture (3 hours estradiol treatment, in red). Aged culture produced more small microcolonies than a not aged culture. It is remarkable that more than 75% of the cells in this aged culture had a replicative age between 1 and 5, which means they were not extremely old cells. A chi square test was realized. and a *p value* inferior to 10^{-6} was obtained.

Small microcolony type	Number of small microcolonies	Founder cell type	Number of small microcolonies
Isotropic growth	83	**Newborn**	39
		Non-newborn	44
Anisotropic growth	10	**Newborn**	1
		Non-newborn	9

Table 1. Number of small microcolonies that presents an anisotropic growth, or an isotropic growth type. Small microcolonies are classified as “isotropic” when all cells within that microcolony divide equally. They are classified as “anisotropic” when one cell (that can be the founder, or first-born cell) produces almost all the divisions within the small microcolony. Either new-borns founder cells or more replicative aged founders, are represented equally in both kinds of growth small microcolonies.

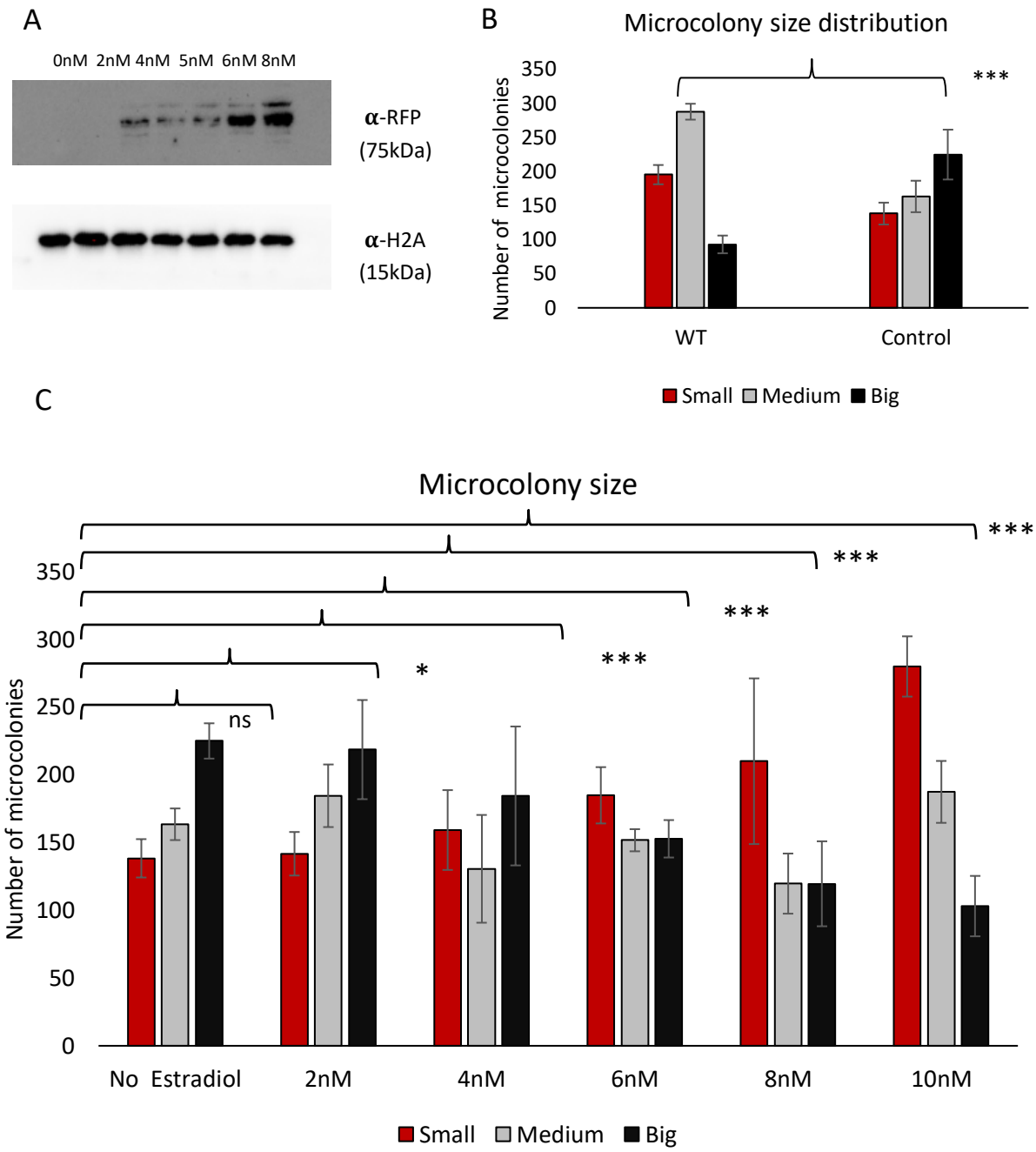

Figure 3. Increasing Whi5 concentration in an inducible Whi5 strain (A) Western Blot of inducible Whi5 strain at different estradiol concentration. This confirms the Whi5 accumulation according to the increasing concentration of estradiol in the media. **(B)** Microcolony size distribution analysis of a WT strain and the KSY098 control without estradiol. Compared to the wildtype profile, the conditional deletion of Whi5 when there is no estradiol in the media produces an

increase in big microcolonies (black) and a decrease in small microcolonies (red). The p value obtained after a chi square test was equal to 10^{-5}. **(C)** Microcolonies size distribution profile of KSY098 strain cultured without estradiol (control), or with 2, 4, 5, 6, 8 or 10nM, respectively. As estradiol concentration increases, expression levels of whi5 get proportionally higher, which produces a progressive raise in the proportion of small microcolonies. A square chi test was performed with the following p values as result (in order left to right): 0,22; 0,038; 10^{-6}; 5,3 *10-^{4}; 10^{-6} and 10^{-6}.

A

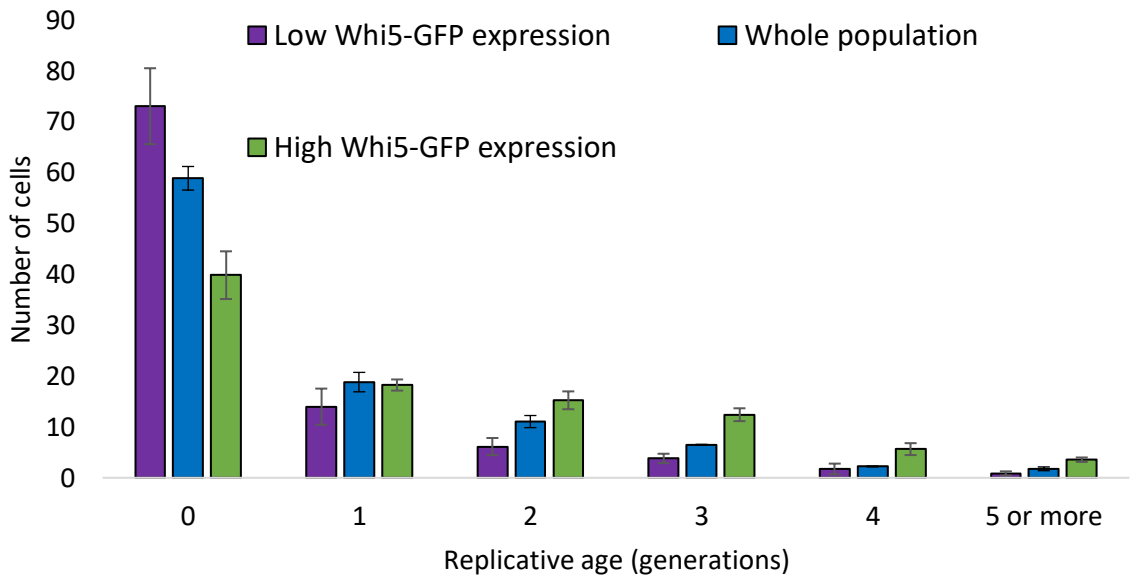
Low Whi5-GFP expression
Whole population
High Whi5-GFP expression
Number of cells
90
80
70
60
50
40
30
20
10
0
0
1
2
3
4
5 or more
Replicative age (generations)

B

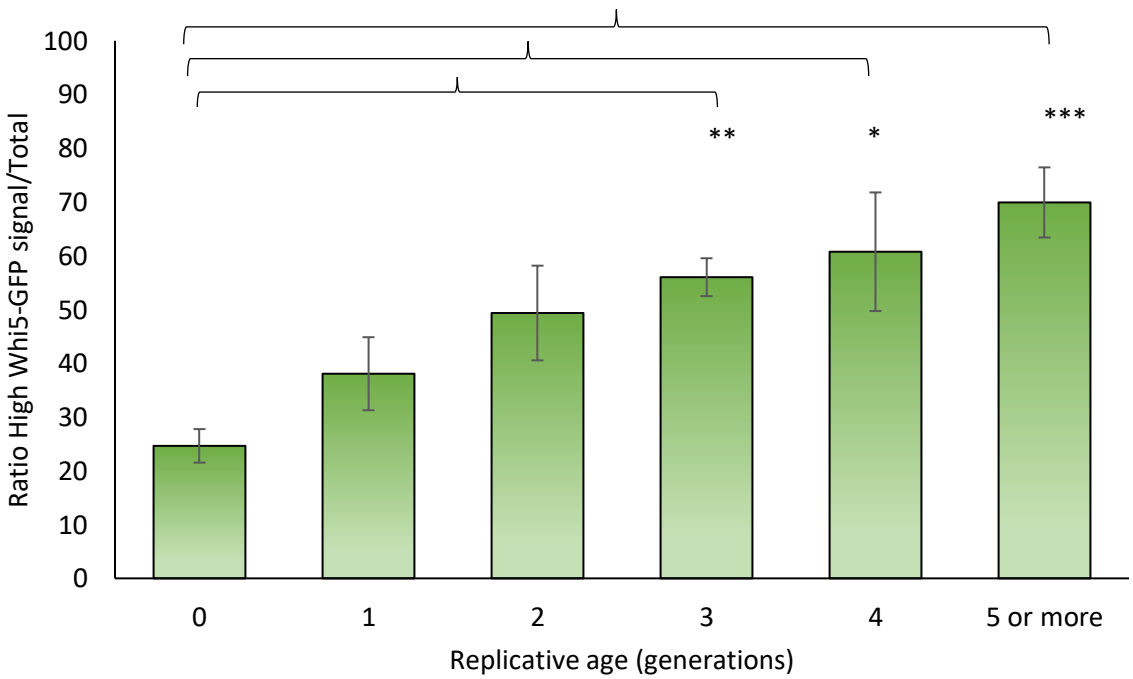
Ratio High Whi5-GFP signal/Total
100
90
80
70
60
50
40
30
20
10
0
**
*
***
0
1
2
3
4
5 or more
Replicative age (generations)

Figure 4. Whi5 expression in cells according to their replicative age. (A) Replicative age distribution, represented as the number of bud scars, for low Whi5 expression sample(purple), whole population (blue) and high Whi5 expression (green). The proportion of cells with higher Whi5 expression changes with the replicative age of the cell: cells with higher number of bud scars frequently have higher Whi5 expression. A Chi square test was performed between low Whi5-GFP expressions cells and High Whi5-GFP expression, with a p value result of 0,02. **(B)** Proportion of cells with higher Whi5 expression found for each replicative age group (represented as the number of bud scars). It is remarkable that cells that have undergone more divisions, also have higher Whi5 expression levels, compare to virgin cells (0 bud scars). A t test was performed with a p value result of $2,6*10^{-3}$, 0,034 and 0,0033 respectively.